effective neutrophil differentiation systems are required to investigate the pathogenesis of various hematological conditions that affect neutrophils using human iPS cells (hiPSCs).

Recent reports describe in vitro culture systems for neutrophil differentiation from hESCs (Choi et al., 2009; Saeki et al., 2009; Yokoyama et al., 2009); however, neutrophil differentiation from hiPSCs has not yet been reported in detail. One of these studies demonstrated that myeloid differentiation could be induced from hiPSCs using the same methodology employed for their differentiation from hESCs (Choi et al., 2009), but the differentiation process and the functions of hiPSC-derived neutrophils were not shown in detail. A system for erythroid differentiation from primate ES and murine iPS cells by co-culture with OP9 stromal cells was developed in previous studies (Umeda et al., 2004; Umeda et al., 2006; Shinoda et al., 2007; Niwa et al., 2009). In the present study, a neutrophil differentiation system from hiPSCs was established by modifying the erythroid differentiation system, and the functions of the hiPSC-derived neutrophils and their differentiation process were analyzed in detail. This system may contribute to the elucidation of the pathogenesis of various blood diseases and the development of novel therapeutic approaches.

Materials and Methods
Maintenance of cells

The human iPS cell lines 201B6, 253G1 and 253G4 were a kind gift from Dr. Yamanaka (Kyoto University, Kyoto), and were generated from human dermal fibroblasts by retrovirus-mediated transfection of four (201B6) or three (253G1 and 253G4) transcription factors (Oct3/4, Sox2, and Klf4, with or without c-Myc) (Takahashi et al., 2007; Nakagawa et al., 2008). The human iPS cell lines and the human ES cell line KhES3-EGFPneo (KhES-3G) were maintained on mitomycin-C (Kyowa Hakko Kirin, Tokyo, Japan) -treated mouse embryonic fibroblasts (MEFs) in DMEM/F12 (Sigma-Aldrich, St. Louis, MO) supplemented with 20% Knockout^{TM} Serum Replacement (Invitrogen, Carlsbad, CA), 5 ng/ml basic fibroblast growth factor (bFGF; R&D Systems, Minneapolis, MN), 1% non-essential amino acids solution (Invitrogen), 5 mM sodium hydroxide solution, 100 μM 2-mercaptethanol, and 2 mM L-glutamine. The culture medium was replaced daily with fresh medium. Colonies were passaged onto new MEFs every 3 or 4 days. The human ES cell line was used in conformity with The Guidelines for Derivation and Utilization of Human Embryonic Stem Cells of the Ministry of Education, Culture, Sports, Science, and Technology, Japan. OP9 stromal cells, which were a kind gift from Dr. Kodama (Osaka University, Osaka), were maintained in α-MEM (Invitrogen) supplemented with 20% fetal calf serum (FCS; Biological Industries, Bet Haemek, Israel).

Antibodies

The antibodies used for flow cytometric analysis included fluorescein isothiocyanate (FITC)-conjugated anti-human TRA 1-85 (R&D Systems), CD45 (Becton-Dickinson, Franklin Lakes, NJ) antibodies, phycoerythrin (PE)-conjugated anti-human CD11b, CD34 (Beckman Coulter, Fullerton, CA), CD13, CD16, CD33 (Becton-Dickinson) antibodies, and allophycocyanin (APC)-conjugated anti-human vascular endothelial growth factor receptor-2 (VEGFR-2) (eBioscience, San Diego, CA) antibody. The primary antibodies used for immunocytochemical analysis included goat anti-human lactoferrin (Santa Cruz Biotechnology, Santa Cruz, CA) and rabbit anti-human MMP9 (Abcam, Cambridge, UK). Biotinylated horse anti-goat or anti-rabbit antibodies (Vector Laboratories, Burlingame, CA) were used as secondary antibodies.

Differentiation of iPS cells

Methods used for the initial differentiation of iPS cells and cell sorting were based on earlier reports (Umeda et al., 2004, 2006). Briefly, trypsin-treated undifferentiated iPS cells were transferred onto OP9 cells and cultured with 20 ng/ml vascular endothelial growth factor (VEGF) (R&D Systems). After 10 days, the induced cells were harvested with cell dissociation buffer (Invitrogen), and sorted TRA 1-85$^+$CD34$^+$VEGFR-2^{high} cells were transferred onto fresh OP9 cells in six-well plates at a concentration of 3 × 10^3 cells per well. Sorted cells were cultured in α-MEM (Invitrogen) containing 10% FCS (Sigma, St Louis, MO), 50 μM 2-mercaptoethanol, 20 ng/ml interleukin (IL)-3, 100 ng/ml stem cell factor (SCF) (R&D Systems), and 10 ng/ml thrombopoietin (TPO) for 20 days. On day 20 after cell sorting, cytokines were changed into 20 ng/ml IL-3 and 10 ng/ml granulocyte colony-stimulating factor (G-CSF). IL-3, TPO and G-CSF were kindly provided by Kyowa Hakko Kirin.

Flow cytometric analysis and cell sorting

Cells were trypsinized and stained with antibodies. Dead cells were excluded by 4',6-diamidino-2-phenylindole (DAPI) staining. Samples were analyzed using an LSR flow cytometer and Cell Quest software (Becton Dickinson). Cell sorting was performed using a FACSVantage SE flow cytometer (Becton Dickinson).

Cytostaining

Floating cells were centrifuged onto glass slides using a Shandon Cytospin® 4 Cytocentrifuge (Thermo, Pittsburgh, PA), and analyzed by microscopy after May–Giemsa, myeloperoxidase (MPO), or alkaline-phosphatase staining. Sequential morphological analysis was performed as follows: all adherent cells including OP9 cells were trypsinized, harvested, and incubated in a new tissue-culture dish (Becton-Dickinson) for 1 h to eliminate adherent OP9 cells (Suwabe et al., 1998). Floating cells were then collected, centrifuged onto glass slides, and analyzed by microscopy after May–Giemsa staining. For immunocytochemical analysis, cells were fixed with 4% paraformaldehyde (PFA), immersed in citrate buffer, and autoclaved for 5 min at 121°C for antigen retrieval (Toda et al., 1999). The slides were then incubated with primary antibodies followed by application of the streptavidinbiotin complex immunoperoxidase technique with diaminobenzidine as chromogen, and nuclei were counterstained with hematoxylin.

Electron microscopy

Cells were fixed in 2% glutaraldehyde in 0.1 M phosphate buffer (PB) for at least 2 h, and then postfixed in 1% osmium tetroxide in 0.1 M PB for 1.5 h. After fixation, samples were dehydrated in a graded ethanol series, cleared with propylene oxide, and embedded in Epon. Thin sections of cured samples were stained with uranyl acetate and Reynolds lead citrate. The sections were inspected using a transmission electron microscope, H7650 (Hitachi, Tokyo, Japan).

Chemotaxis assay

Chemotactic ability was determined using a modified Boyden chamber method (Boyden, 1962; Harvath et al., 1980). Briefly, 500 μl of the reaction medium (Hank's Balanced Salt Solution (HBSS) containing 2.5% FCS) with or without 10 nM formyl-Met-Leu-Phe (fMLP; Sigma-Aldrich) was placed into each well of a 24-well plate, and the cell culture insert (3.0-μm pores; Becton Dickinson) was gently placed into each well to divide the well into upper and lower sections. Floating cells were suspended in the reaction medium at 7.0 × 10^4/ml, and a 500-μl cell suspension was added to the upper well, allowing the cells to migrate from the upper to the lower side of the membrane for 4 h at 37°C. After incubation, cells in the lower chamber were collected and counted using an LSR flow cytometer. Cells were counted by flow cytometry as follows:

equivalent amounts of counting beads were added to each sample and counted until the bead count reached 10,000.

MPO activity assay

The EnzChek Myeloperoxidase (MPO) Activity Assay Kit (Molecular Probes, Leiden, The Netherlands) was used for rapid and sensitive determination of MPO chlorination activity in cell lysates. The procedure was performed following the manufacturer's instructions. Cell lysate samples were prepared from 1×10^4 floating cells by freeze-thaw cycles. Fluorescence was measured with a fluorescence microplate reader (Wallac 1420 ARVO sx; PerkinElmer, Waltham, MA) using fluorescence excitation and emission at 485 and 530 nm, respectively. The background fluorescence measured for each zero-MPO control reaction was subtracted from each fluorescence measurement before plotting.

DHR assay

Neutrophil production of reactive oxygen species was detected by flow cytometry using dihydrorhodamine 123 (DHR) as described previously (Vowells et al., 1995). Briefly, 3.5×10^4 floating cells were suspended in 100 μl of the reaction buffer (HBSS containing 0.1% FCS and 5 mM glucose) per tube, and two tubes were prepared for each sample. Catalase (Sigma-Aldrich) at a final concentration of 1000 U/ml and DHR at a final concentration of 1.0×10^5 nM were added and incubated for 5 min in a 37°C shaking water bath. After incubation, phorbol myristate acetate (PMA; Sigma-Aldrich) at a final concentration of 400 ng/ml was added to one of the two tubes and tubes were returned to the water bath for an additional 15 min. Following incubation, rhodamine fluorescence from the oxidized DHR was detected using an LSR flow cytometer.

Phagocytosis and detection of reactive oxygen species

Phagocytosis and neutrophil production of reactive oxygen species was detected by chemiluminescent microspheres (luminol-binding carboxyl hydrophilic microspheres; TORAY, Tokyo, Japan) as described previously (Uchida et al., 1985). Briefly, 2×10^4 floating cells were suspended in 50 μl of the reaction buffer (HBSS containing 20 mM N-2-hydroxyethylpiperazine-N'-2-ethanesulfonic acid (HEPES)) per tube. To activate the system, 5 μl of chemiluminescent microspheres was added, and light emission was recorded continuously. During the measurement, samples were kept at 37°C. To inhibit the phagocytosis, 1.75 μg of cytochalasin B (Sigma-Aldrich) was added to the sample. Chemiluminescence from the microspheres was detected using a luminometer (TD-20/20; Turner Designs, Sunnyvale, CA).

RNA extraction and RT-PCR analysis

RNA samples were prepared using silica gel membrane-based spin-columns (RNeasy Mini-Kit™, Qiagen, Valencia, CA) and subjected to reverse transcription (RT) with the Ominscript-RT Kit™ (Qiagen). All procedures were performed following the manufacturer's instructions. For reverse transcriptase-polymerase chain reaction (RT-PCR), yields were adjusted by dilution to produce equal amounts of the human glyceraldehyde-3-phosphate dehydrogenase (GAPDH) amplicon. The complementary DNA (cDNA) templates were initially denatured at 94°C for 5 min, followed by 30–40 amplification reactions consisting of 94°C for 15–30 sec (denaturing), 55–63°C for 15–30 sec (annealing), and 72°C for 30–60 sec (extension), with a final extension at 72°C for 7 min. The oligonucleotide primers were as follows: NANOG, 5′-CAG CCC TGA TTC TTC CAC CAG TCC C-3′ and 5′-TGG AAG GTT CCC AGT CGG GTT CAC C-3′ (Takahashi et al., 2007); human GAPDH, 5′-CAC CAG GGC TGC TTT TAA CTC TG-3′ and 5′-ATG GTT CAC ACC CAT GAC GAA C-3′ (Umeda et al., 2006); PU.1, 5′-CTG CAT TGG CCC CCA CCG AG-3′ and 5′-AGG TCT TCT GAT GGC TGA GGG GG-3′; C/EBPα, 5′-TAA CCT TGT GCC TTG GAA ATG CAA AC-3′ and 5′- ATG TTT

CCA CCC CTT TCT AAG GAC A-3′ (Duan and Horwitz, 2003); C/EBPε, 5′- AGT CTG GGG AAG AGC AGC TTC-3′ and 5′- ACA GTG TGC CAC TTG GTA CTG-3′ (Mori et al., 2009); MPO, 5′-TGA GGA CGG CTT CTC TCT TC-3′ and 5′-CCC GGT AAG TGA TGA TCT GG-3′; Lactoferrin, 5′-AGC TGG CAG ACT TTG CGC T-3′ and 5′-TTC AGA TTA GTA ATG CCT GCG ACA TAC-3′ (Kholodnyuk et al., 2006); Gelatinase (MMP-9), 5′-GCC TCC AAC CAC CAC CAC AC-3′ and 5′-GCC CAG CCC ACC TCC ACT C-3′ (Sugimoto et al., 2001); mouse GAPDH, 5′-ACG GCC GCA TCT TCT TGT GCA-3′ and 5′-CAC CCT TCA AGT GGG CCC CG-3′. PCR amplification reaction cycles were performed in the linear range for each primer by carrying out primer titrations. The number of reaction cycles per sample were: NANOG, 35 cycles; human GAPDH, 30 cycles; PU.1, 40 cycles; C/EBPα, 40 cycles; C/EBPε, 40 cycles; MPO, 35 cycles; Lactoferrin, 35 cycles; Gelatinase (MMP-9), 40 cycles; mouse GAPDH, 30 cycles.

Statistics

Statistical analyses were conducted using the Student's t-test. Statistical significance was defined as $P < 0.05$.

Results

Neutrophil differentiation from hiPSCs in co-culture with OP9 stromal cells

A culture system for the induction of erythroid cell differentiation from primate ES and murine iPS cells by co-culture with OP9 stromal cells (Umeda et al., 2004; Umeda et al., 2006; Shinoda et al., 2007; Niwa et al., 2009) was established, and this system was applied for neutrophil differentiation from hiPSCs. Prior data in primate ES cells suggested that the VEGFR-2^{high} fraction of differentiated cells contained hemangioblasts and VEGFR-2^{high}CD34$^+$ cells had more hematopoietic potential (Umeda et al., 2006). Therefore, the expression of VEGFR-2 and CD34 was examined using three human iPS cell lines (201B6, 253G1, 253G4) and one ES cell line (KhES-3G). After 10 days of co-culture with OP9 in the presence of 20 ng/ml VEGF, VEGFR-2^{high}CD34$^+$ cells appeared from all hiPSC lines in a similar manner to the ES cell line (Fig. 1A). Among these three human iPS cell lines, the highest percentage of VEGFR-2^{high}CD34$^+$ cells was detected in 253G4 (Fig. 1B), and the data on this cell line is therefore presented below.

The VEGFR-2^{high}CD34$^+$ cell fraction was sorted (Fig. 1C) and 1.1×10^4 (range; 0.6–2.2 $\times$ 10^4 in 14 independent cultures) VEGFR-2^{high}CD34$^+$ cells were grown in one 10-cm dish containing hiPSCs. They were then transferred onto fresh OP9 cells and cultured in the presence of hematopoietic cytokines. Around 10 days after cell sorting (day 10 + 10), small, round cell colonies appeared (Fig. 1D), and these colonies gradually grew in both size and number (Fig. 1E). At the same time, floating cells also appeared, and the average number of floating cells from 1×10^4 sorted VEGFR-2^{high}CD34$^+$ cells at 30 days after cell sorting (day 10 + 30) was 4.1×10^4 (range; 0.2–9.9 $\times$ 10^4 in 11 independent cultures).

May–Giemsa staining of the floating cells on day 10 + 30 revealed that 38.0 ± 1.6% of the cells were stab and segmented neutrophils (Fig. 1F), which were positive for MPO (Fig. 1G) and neutrophil alkaline-phosphatase (Fig. 1H). The rest were mainly immature myeloid cells and a small number of macrophages, and cells of other lineages, such as erythroid or lymphoid cells, were not observed. The frequency of MPO- and neutrophil alkaline-phosphatase-positive cells is shown in Table 1. The results were consistent with the morphological features revealed by May–Giemsa staining.

Surface marker analysis revealed that these floating cells were positive for CD45 and CD11b, and partially positive for CD13, CD33, and CD16 (Fig. 1I). The expression pattern of these surface markers was similar to that of neutrophils or immature myeloid cells in healthy bone marrow (van Lochem et al., 2004), although the CD16 expression level was lower.
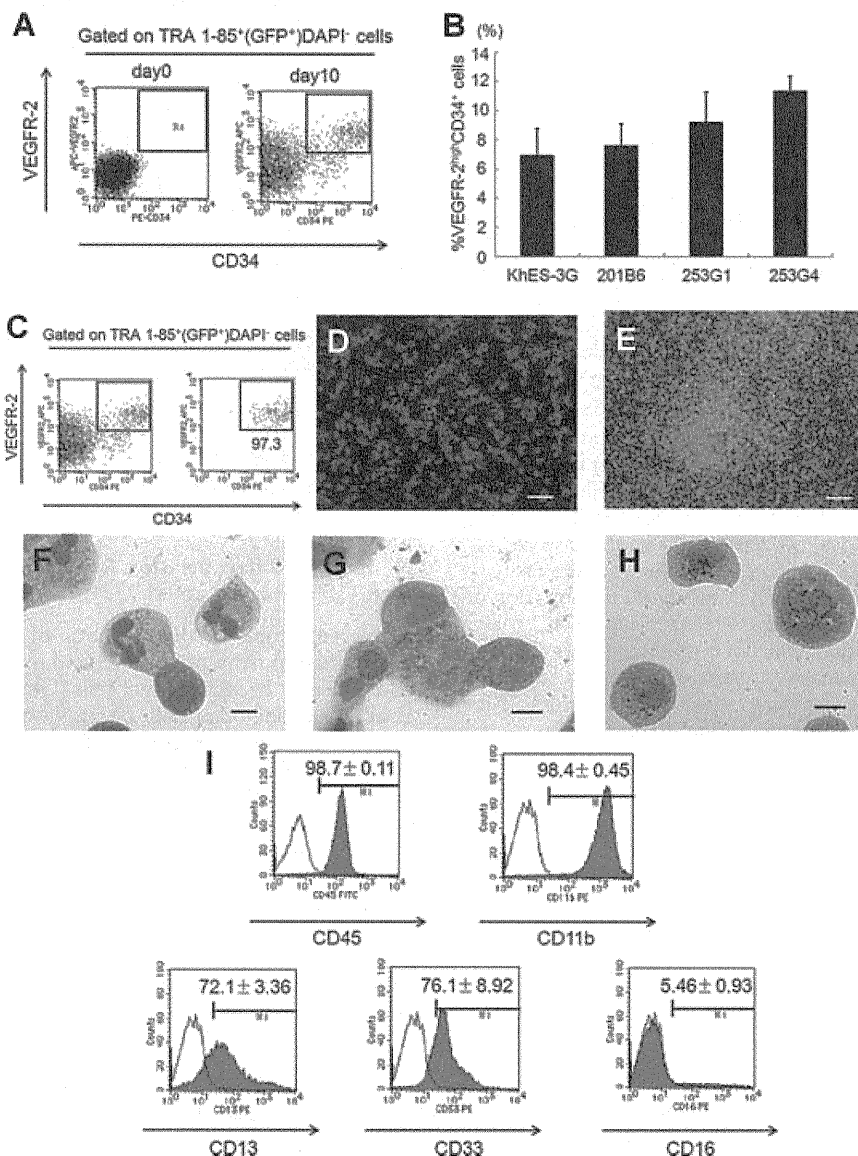
Fig. 1. Neutrophil differentiation from hiPSCs in co-culture with OP9 stromal cells. (A–B) Flow cytometric analysis of VEGFR-2 and CD34 during differentiation induction. TRA 1-85$^+$ (GFP$^+$) DAPI$^-$ cells were gated as human iPS (ES) cell-derived viable cells. Undifferentiated iPS (ES) cells and 10-day culture cells were stained with antibodies specific for VEGFR-2 and CD34. Representative results from one of three independent experiments (A) and percentages of VEGFR-2^{high}CD34$^+$ cells on day 10 (B) are shown (n = 3; bars represent SDs). (C) VEGFR-2^{high}CD34$^+$ cells were sorted on day 10. Representative dot plots and percentages of gated cells are shown. Purities of viable VEGFR-2^{high}CD34$^+$ cells were calculated at 95.5 ± 1.9% from 14 independent experiments. (D–E) Micrographs of adherent hematopoietic cell clusters generated on day 10 (D) and day 30 (E) after cell sorting. Scale bars: 200 μm. (F–H) May–Giemsa staining (F), myeloperoxidase staining (G), and neutrophil alkaline-phosphatase staining (H) of floating cells on day 10 + 30. Scale bars: 10 μm. (I) Flow cytometric analysis of floating cells on day 10 + 30 were stained with antibodies specific for CD45, CD11b, CD13, CD33, or CD16. Plots show the negative control profile (open bars) versus the specific antibody staining profiles (shaded bars). Representative results from one of three independent experiments are shown. [Color figure can be viewed in the online issue, which is available at wileyonlinelibrary.com.]

TABLE 1. Frequency of staining-positive cells for neutrophil specific granules

Staining	Frequency of positive cells (%)
Myeloperoxidase	93.7 ± 1.7
Neutrophil alkaline-phosphatase	39.0 ± 2.2
Lactoferrin	79.0 ± 1.4
Gelatinase	59.0 ± 3.7

Data are shown as mean ± SD (n = 3 independent experiments).

This lower CD16 expression level was similar to that of neutrophils derived in vitro from bone marrow CD34$^+$ cells by stimulation with G-CSF (Kerst et al., 1993b) and to the effect in vivo when G-CSF is administered to healthy volunteers (Kerst et al., 1993a). These results indicated that the modified OP9 co-culture system could differentiate mature neutrophils from immature hiPSCs.

hiPSC-derived neutrophils contain neutrophil specific granules

Mature neutrophils in vivo have intracellular granules that are important for their bactericidal function. The granules can be

classified into three types based on their size, morphology, or electron density, or with reference to a given protein: primary (azurophilic) granules contain MPO, secondary granules contain lactoferrin, and tertiary granules contain gelatinase (Borregaard and Cowland, 1997).

To assess the presence of these granules in hiPSC-derived neutrophils, they were imaged using transmission electron microscopy, which showed that the hiPSC-derived mature neutrophils contained peroxidase-positive and negative granules, as was observed in peripheral blood neutrophils (Fig. 2A–B). Immunocytochemical analysis revealed that hiPSC-derived mature neutrophils were also positive for lactoferrin and gelatinase (Fig. 2C–D). The frequencies of cells that were positive for neutrophil specific granules, as observed by transmission electron microscopy (Table 2) and immunocytochemical analysis (Table 1), were more than 90% for primary granules, about 80% for secondary granules, and approximately 60% for tertiary granules. These results indicated that hiPSC-derived neutrophils contained neutrophils-specific granules.

hiPSC-derived neutrophils exhibit biological bactericidal activities

Because neutrophils patrol circulating blood and play a key role in early phase defense mechanisms, the chemotactic, phagocytotic, and bactericidal activities of hiPSC-derived neutrophils were analyzed.

Chemotactic activity was assessed using a modified Boyden chamber method (Boyden, 1962; Harvath et al., 1980). After incubation with or without fMLP in the lower well, neutrophils had migrated from the upper side to the lower side of the membrane. Incubation with fMLP caused an increase in the number of migrated cells of more than three times compared to cells without fMLP, suggesting that hiPSC-derived neutrophils had chemotactic activity in response to a chemoattractant similar to natural neutrophils derived from bone marrow (Fig. 3A).

The MPO-dependent chlorination activity and reactive oxygen production of hiPSC-derived neutrophils, which are

TABLE 2. Frequency of positive cells for neutrophil specific granules under transmission electron microscopy

Granules	Frequency of positive cells (%)
Peroxidase-positive granules	95.1 (135/142)
Peroxidase-negative granules	86.6 (123/142)

both essential for their bactericidal function, were determined next. MPO reacts with hydrogen peroxide (H_2O_2) to form the active redox and enzyme intermediate compound MPO-I, which oxidizes chloride (Cl^-) to HOCl (Winterbourn, 2002). As shown in Figure 3B, hiPSC-derived neutrophils showed MPO-dependent chlorination activity. To evaluate reactive oxygen production, the ability to convert DHR to rhodamine was assessed using flow cytometry (Vowells et al., 1995) and the results revealed that hiPSC-derived neutrophils characteristically produced superoxide in response to PMA (Fig. 3C).

Finally, phagocytotic activity and phagosome-dependent reactive oxygen production were measured using luminol-bound microspheres (Uchida et al., 1985). As shown in Figure 3D, the captured data confirmed that hiPSC-derived neutrophils could produce reactive oxygen species in response to the phagocytosis of microspheres, which was completely abolished in the presence of the antiphagocytic agent cytochalasin B. Moreover, transmission electron microscopy successfully captured a screenshot of a neutrophil phagocytosing the microbeads (Fig. 3E). The above results clearly show that neutrophils derived from hiPSC using the present culture system maintain their functional status.

Step-wise neutrophil differentiation from hiPSCs is similar to normal granulopoiesis

Disorders of neutrophil differentiation are observed in various hematological diseases, among them the maturation arrest of neutrophil precursors in the bone marrow at the promyelocyte stage in severe congenital neutropenia. Thus, in clinical applications for disease investigation, the sequential analysis of the differentiation process from hiPSC to mature neutrophils in this culture system is required.

Observation of the sequential changes in cell morphology was done using May–Giemsa staining. Visualization of the morphology of day10 + 10 cells revealed that the cells were mainly myeloblasts and promyelocytes (Fig. 4A). On day10 + 20, myelocytes and metamyelocytes became predominant (Fig. 4B), and on day 10 + 30, stab and segmented neutrophils became predominant (Fig. 4C).

Surface antigen expression at each differentiation stage of hiPSC-derived cells was analyzed by flow cytometry (Fig. 4D). CD34, cell surface marker on normal immature hematopoietic cells, was detected in about 20% of the cells on day 10 + 10, but disappeared gradually thereafter. From day 10 + 10 to 10 + 30, the common myeloid antigens CD11b and CD33 were expressed in almost all the cells. Interestingly, expression of CD13, also a common myeloid antigen, was observed in less than 20% of cells at day 10 + 10 and did not subsequently increase. The expression level of CD16, which is a representative marker of matured neutrophils (van de Winkel and Anderson, 1991), doubled from day 10 + 10 to day 10 + 20, although the increase in expression was not statistically significant. These expression patterns were consistent with the patterns observed during normal neutrophil differentiation in healthy bone marrow (van Lochem et al., 2004).

The gene expression patterns of the pluripotency marker, transcription factors and granule proteins during neutrophil
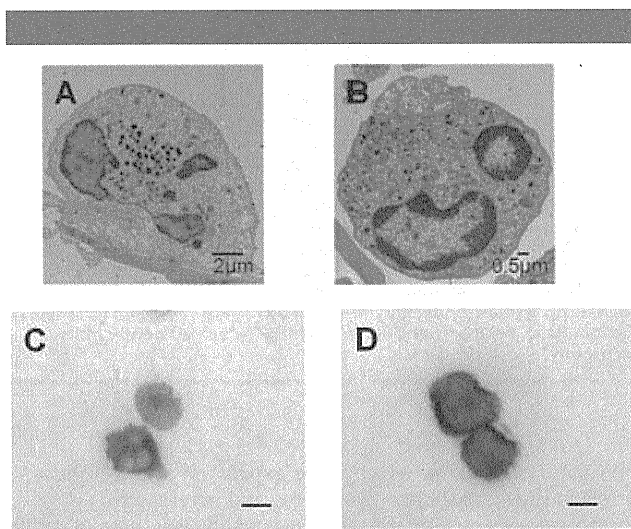

Fig. 2. Neutrophil-specific granules in hiPSC-derived neutrophils. (A–B) Floating cells on day10 + 30 (A) and peripheral blood neutrophils (B) were analyzed by transmission electron microscope. **(C–D)** Immunocytochemical analysis. Floating cells on day10 + 30 were stained for lactoferrin (C) and MMP9 (gelatinase) (D). Scale bars: 10 μm. [Color figure can be viewed in the online issue, which is available at wileyonlinelibrary.com.]
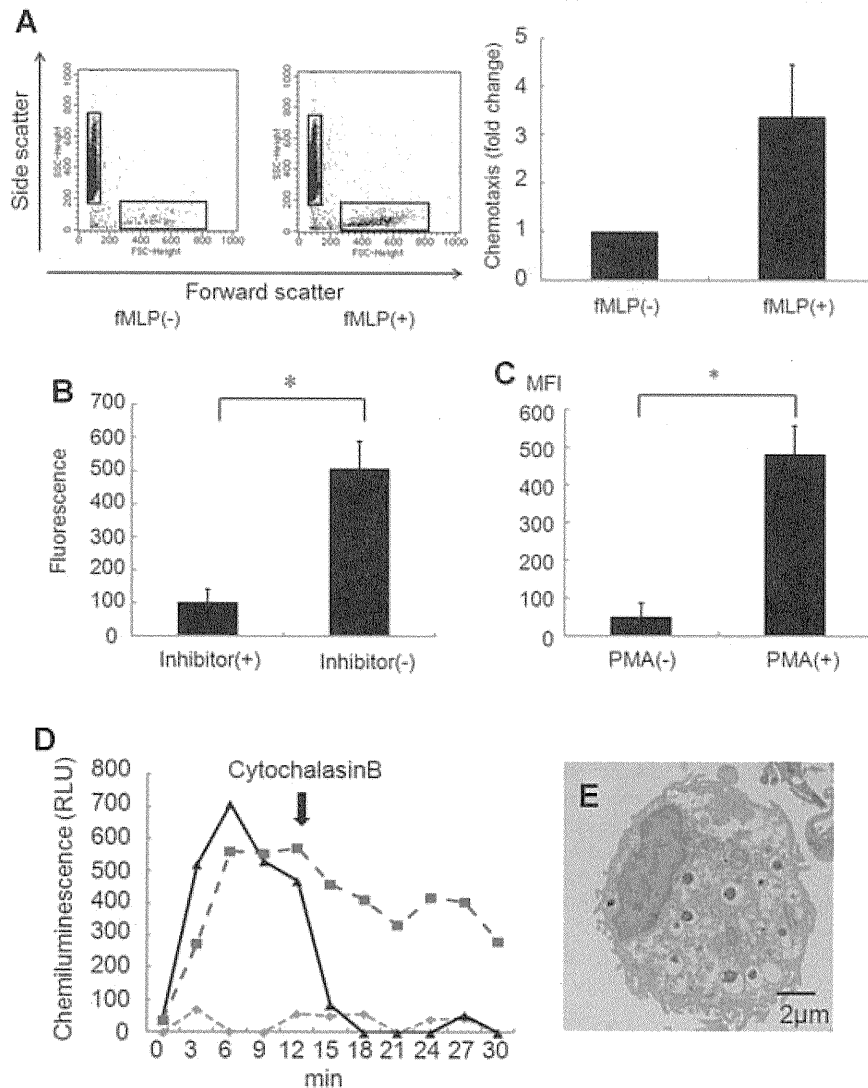
Fig. 3. Functional analysis of hiPSC-derived neutrophils. (A) Chemotactic activity of floating cells on day10 + 30 in response to fMLP was determined as described in Materials and Methods section. After a 4-h culture, the transwell inserts were removed, and the cells in the lower chamber were counted by an LSR flow cytometer (n = 3; bars represent SDs). (B) MPO chlorination activity in cell lysates from floating cells on day10 + 30 was analyzed by EnzChek Myeloperoxidase (MPO) Activity Assay Kit as described in the Materials and Methods section. The chlorination activity in neutrophil cell lysates was almost completely abolished by the addition of a chlorination inhibitor (n = 3; bars represent SDs; *P < 0.05.). (C) Floating cells on day10 + 30 were subjected to DHR assay. DHR was reacted with neutrophils with or without PMA, and the resultant rhodamine fluorescence was detected by flow cytometry. The addition of PMA increased the levels of fluorescence. Results are expressed as mean fluorescence intensity (MFI) (n = 3; bars represent SDs; *P < 0.05.). (D) Floating cells on day10 + 30 were subjected to the assay for phagocytosis-induced respiratory burst activity using chemiluminescent microspheres (luminol-binding microspheres). Gradual increase in chemiluminescence indicates the respiratory burst triggered by the phagocytosis of luminol-binding microspheres (squares). The increase in chemiluminescence was almost completely abolished by the addition of cytochalasin B (diamonds) and inhibited by its later addition (triangles). The figures are representative of three independent experiments. Abbreviation: RLU, relative light units. (E) hiPSC-derived neutrophils phagocytosing the microbeads were analyzed by transmission electron microscopy.

differentiation in this culture system were investigated by RT-PCR (Fig. 4E–F). NANOG, a pluripotency marker, was expressed in undifferentiated iPS cells but disappeared in sorted VEGFR2highCD34+ cells after 10 days differentiation. PU.1 and C/EBPα, essential transcription factors for commitment and differentiation of the granulocytic lineage (Borregaard et al., 2001; Friedman, 2007) were first detected on day 10 + 10 and persisted thereafter. C/EBPε, which had a critical role for the later stages of neutrophil development and transcription of key granule proteins (Borregaard et al., 2001; Friedman, 2007) were first detected faintly on day 10 + 10 and upregulated thereafter.

MPO and lactoferrin, which were expressed at the highest levels in myeloblasts/promyelocytes and myelocytes/metamyelocytes, respectively (Cowland and Borregaard, 1999; Borregaard et al., 2001), were detected on day 10 + 10. Gelatinase, which was expressed at the highest level in band and segmented neutrophilic cells (Cowland and Borregaard, 1999; Borregaard et al., 2001), was first detected on day 10 + 20 and upregulated thereafter. Altogether, these results suggested that the neutrophil differentiation in this co-culture system might recapitulate the orderly differentiation process in bone marrow.
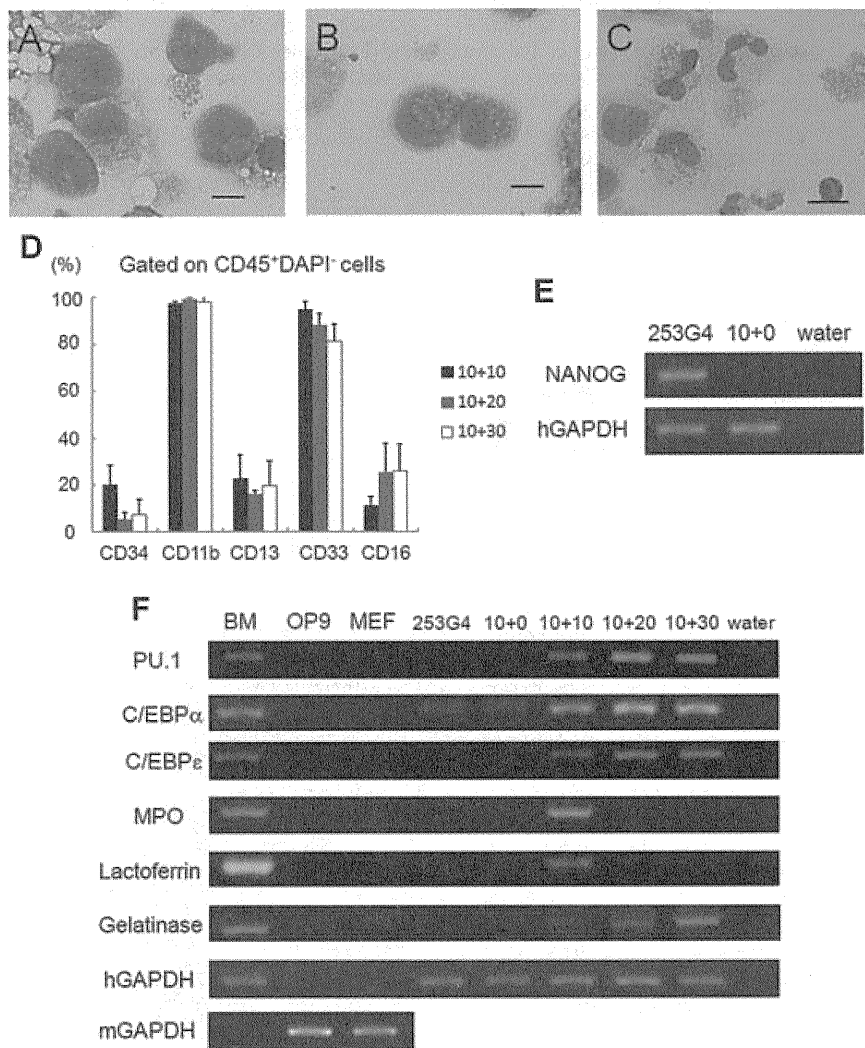
Fig. 4. Sequential analysis of neutrophil differentiation from hiPSCs. (A–C) Sequential morphological analysis of day 10 + 10 (A), day 10 + 20 (B) and day 10 + 30 (C). Scale bars: 10 μm. (D) Surface antigen expression at each level of differentiation of hiPSC-derived cells was analyzed by flow cytometry. All adherent cells including OP9 cells were harvested and stained with antibodies. Human CD45$^+$DAPI$^-$ cells were gated as hiPSC-derived viable leukocytes (n = 3; bars represent SDs). (E–F) Sequential RT-PCR analysis of a pluripotency marker (E), genes associated with neutrophil development and neutrophils-specific granules (F) during differentiation. Human GAPDH was used as a loading control. Abbreviations: BM, human bone marrow cells; 253G4, undifferentiated 253G4 cells; 10 + 0, sorted VEGFR2^{high}CD34$^+$ cells after 10 days differentiation; 10 + 10, 20, 30, all cells after 10, 20, 30 days differentiation after cell sorting; hGAPDH, human GAPDH; mGAPDH, mouse GAPDH. The figures are representative of three independent experiments. [Color figure can be viewed in the online issue, which is available at wileyonlinelibrary.com.]

Discussion

The analysis of the differentiation process of neutrophils can provide helpful information for the elucidation of the pathogenesis of hematopoietic diseases that affect neutrophils and/or myeloid differentiation, including inherited bone marrow failure syndromes and neutrophil function disorders. Traditionally, HL-60, an acute promyelocytic cell line, has been used as a neutrophil differentiation model (Collins et al., 1978; Newburger et al., 1979). Although this cell line grows well and differentiates easily into neutrophils, the neutrophil differentiation model is not suitable for the analysis of neutrophil-affected disorders because of its leukemic cell-origin. Development of a neutrophil differentiation system based on iPS cells would provide a better model for the analysis of such diseases, because iPS cells can be generated from the somatic cells of patients suffering from these diseases.

The current study aimed to investigate two issues in hiPSC-derived neutrophil differentiation: tracking the step-wise maturation in vitro and evaluating the wide spectrum of neutrophil functions. Through the use of a modified OP9 co-culture system, the directed and step-wise differentiation from hiPSCs to mature neutrophils containing neutrophil specific granules was first accomplished. The expression of surface antigens, transcription factors and granule proteins during differentiation exhibited the characteristic pattern of normal granulopoiesis. The biological functions of hiPSC-derived neutrophils were demonstrated through the quantitative assessment of granule enzyme activities and biological bactericidal activities such as chemotaxis and phagocytosis.

Defects in the maturation and function of neutrophils are associated with certain blood diseases including inherited bone marrow failure syndromes and neutrophil function disorders.

Among bone marrow failure syndromes, certain conditions affect a specific maturation stage, such as the maturation arrest at the plomyelocyte/myelocyte stage seen in severe congenital neutropenia. Neutrophil function disorders can affect specific bactericidal activities, such as the absence of MPO activity characteristic of MPO deficiency disorders. The use of hiPSCs for the investigation of these diseases requires sequential analyses that can identify each neutrophil maturation stage and include a functional analysis to evaluate each bactericidal activity separately on disease-specific, iPSC-derived neutrophils. Although previous studies have reported neutrophil differentiation models from hESCs (Choi et al., 2009; Saeki et al., 2009; Yokoyama et al., 2009) and hiPSC-derived neutrophils have been shown before (Choi et al., 2009), evidence showing that hiPSCs, which are artificially reprogrammed somatic cells, can follow the normal developmental pathway into fully functional mature neutrophils is of great significance, and the description of methods for identifying each neutrophil maturation step and analyzing each bactericidal pathway separately is important for clinical applications.

Although flow-cytometric analysis combined with RT-PCR identified the neutrophil maturation step relatively successfully, discrepancies between the neutrophil differentiation system in this study and normal granulopoiesis were noted such as the lower expression of CD16 than that shown by previous reports on hESC-derived neutrophils (Choi et al., 2009; Saeki et al., 2009; Yokoyama et al., 2009). As CD16 is a mature neutrophil marker in peripheral blood, two reasons could explain this phenomenon. First, residual precursors could have been more significant contaminants in the present system than in previously reported methods due to the function of cytokines and stroma supporting immature hematopoietic cells. Another possible reason is the shift of protein types between membrane-bound and soluble forms. Calluri previously reported that G-CSF is not only a myeloid cell growth factor, but also a modulator of neutrophil behavior (Carulli, 1997), and its stimulation decreases the membrane bound CD16 and increases its soluble form. Low CD16 expression has been documented in neutrophils derived in vitro from bone marrow CD34^{+} cells by stimulation with G-CSF (Kerst et al., 1993b), and it has been observed in vivo when G-CSF is administered to healthy volunteers (Kerst et al., 1993a). This phenomenon, which is also documented in a report of hESC-derived neutrophils (Yokoyama et al., 2009), is unavoidable in differentiation culture systems using recombinant cytokines. The combination of flow cytometric and PCR analyses enables a more accurate staging of progenitors that could be of importance in the investigation of maturation arrest in future studies.

The culture system presented in this study is considered ineligible for clinical applications due to the use of xenogeneic factors such as OP9 cells and FCS. To overcome this problem, a xeno-free hematopoietic differentiation system from pluripotent cells is currently being established.

In conclusion, the present study shows the establishment of a fully functional mature neutrophil differentiation system from hiPSCs and the detailed analysis of their function and differentiation process. This system could become a useful tool for the investigation of various hematological diseases with defects in maturation and function of neutrophils.

References

Agarwal S, Loh YH, McLoughlin EM, Huang J, Park IH, Miller JD, Huo H, Okuka M, Dos Reis RM, Loewer S, Ng HH, Keefe DL, Goldman FD, Klingelhutz AJ, Liu L, Daley GQ. 2010. Telomere elongation in induced pluripotent stem cells from dyskeratosis congenita patients. Nature 464:292–296.

Alter BP. 2007. Diagnosis, genetics, and management of inherited bone marrow failure syndromes. Hematology Am Soc Hematol Educ Program 29–39.

Borregaard N, Cowland JB. 1997. Granules of the human neutrophilic polymorphonuclear leukocyte. Blood 89:3503–3521.

Borregaard N, Theilgaard-Monch K, Sorensen OE, Cowland JB. 2001. Regulation of human neutrophil granule protein expression. Curr Opin Hematol 8:23–27.

Boyden S. 1962. The chemotactic effect of mixtures of antibody and antigen on polymorphonuclear leucocytes. J Exp Med 115:453–466.

Carulli G. 1997. Effects of recombinant human granulocyte colony-stimulating factor administration on neutrophil phenotype and functions. Haematologica 82:606–616.

Choi KD, Vodyanik MA, Slukvin II. 2009. Generation of mature human myelomonocytic cells through expansion and differentiation of pluripotent stem cell-derived lin-CD34+CD43+CD45+ progenitors. J Clin Invest 119:2818–2829.

Collins SJ, Ruscetti FW, Gallagher RE, Gallo RC. 1978. Terminal differentiation of human promyelocytic leukemia cells induced by dimethyl sulfoxide and other polar compounds. Proc Natl Acad Sci USA 75:2458–2462.

Cowland JB, Borregaard N. 1999. The individual regulation of granule protein mRNA levels during neutrophil maturation explains the heterogeneity of neutrophil granules. J Leukoc Biol 66:989–995.

Duan Z, Horwitz M. 2003. Targets of the transcriptional repressor oncoprotein Gfi-1. Proc Natl Acad Sci USA 100:5932–5937.

Evans MJ, Kaufman MH. 1981. Establishment in culture of pluripotential cells from mouse embryos. Nature 292:154–156.

Friedman AD. 2007. Transcriptional control of granulocyte and monocyte development. Oncogene 26:6816–6828.

Harvath L, Falk W, Leonard EJ. 1980. Rapid quantitation of neutrophil chemotaxis: use of a polyvinylpyrrolidone-free polycarbonate membrane in a multiwell assembly. J Immunol Methods 37:39–45.

Kerst JM, de Haas M, van der Schoot CE, Slaper-Cortenbach IC, Kleijer M, von dem Borne AE, van Oers RH. 1993a. Recombinant granulocyte colony-stimulating factor administration to healthy volunteers: induction of immunophenotypically and functionally altered neutrophils via an effect on myeloid progenitor cells. Blood 82:3265–3272.

Kerst JM, van de Winkel JG, Evans AH, de Haas M, Slaper-Cortenbach IC, de Wit TP, von dem Borne AE, van der Schoot CE, van Oers RH. 1993b. Granulocyte colony-stimulating factor induces hFc gamma RI (CD64 antigen)-positive neutrophils via an effect on myeloid precursor cells. Blood 81:1457–1464.

Kholodnyuk ID, Kozireva S, Kost-Alimova M, Kashuba V, Klein G, Imreh S. 2006. Down regulation of 3p genes, LTF, SLC38A1 and DRR1, upon growth of human chromosome 3-mouse fibrosarcoma hybrids in severe combined immunodeficiency mice. Int J Cancer 119:99–107.

Lensch MW, Daley GQ. 2006. Scientific and clinical opportunities for modeling blood disorders with embryonic stem cells. Blood 107:2605–2612.

Meissner A, Wernig M, Jaenisch R. 2007. Direct reprogramming of genetically unmodified fibroblasts into pluripotent stem cells. Nat Biotechnol 25:1177–1181.

Mori Y, Iwasaki H, Kohno K, Yoshimoto G, Kikushige Y, Okeda A, Uike N, Niiro H, Takenaka K, Nagafuji K, Miyamoto T, Harada M, Takatsu K, Akashi K. 2009. Identification of the human eosinophil lineage-committed progenitor: revision of phenotypic definition of the human common myeloid progenitor. J Exp Med 206:183–193.

Nakagawa M, Koyanagi M, Tanabe K, Takahashi K, Ichisaka T, Aoi T, Okita K, Mochiduki Y, Takizawa N, Yamanaka S. 2008. Generation of induced pluripotent stem cells without Myc from mouse and human fibroblasts. Nat Biotechnol 26:101–106.

Newburger PE, Chovaniec ME, Greenberger JS, Cohen HJ. 1979. Functional changes in human leukemic cell line HL-60. A model for myeloid differentiation. J Cell Biol 82:315–322.

Niwa A, Umeda K, Chang H, Saito M, Okita K, Takahashi K, Nakagawa M, Yamanaka S, Nakahata T, Heike T. 2009. Orderly hematopoietic development of induced pluripotent stem cells via Flk-1(+) hemoangiogenic progenitors. J Cell Physiol 221:367–377.

Okita K, Ichisaka T, Yamanaka S. 2007. Generation of germline-competent induced pluripotent stem cells. Nature 448:313–317.

Park IH, Arora N, Huo H, Maherali N, Ahfeldt T, Shimamura A, Lensch MW, Cowan C, Hochedlinger K, Daley GQ. 2008a. Disease-specific induced pluripotent stem cells. Cell 134:877–886.

Park IH, Zhao R, West JA, Yabuuchi A, Huo H, Ince TA, Lerou PH, Lensch MW, Daley GQ. 2008b. Reprogramming of human somatic cells to pluripotency with defined factors. Nature 451:141–146.

Raya A, Rodriguez-Piza I, Guenechea G, Vassena R, Navarro S, Barrero MJ, Consiglio A, Castella M, Rio P, Sleep E, Gonzalez F, Tiscornia G, Garreta E, Aasen T, Veiga A, Verma IM, Surralles J, Bueren J, Izpisua Belmonte JC., 2009. Disease-corrected haematopoietic progenitors from Fanconi anaemia induced pluripotent stem cells. Nature 460:53–59.

Saeki K, Nakahara M, Matsuyama S, Nakamura N, Yogiashi Y, Yoneda A, Koyanagi M, Kondo Y, Yuo A. 2009. A feeder-free and efficient production of functional neutrophils from human embryonic stem cells. Stem Cells 27:59–67.

Shinoda G, Umeda K, Heike T, Arai M, Niwa A, Ma F, Suemori H, Luo HY, Chui DH, Torii R, Shibuya M, Nakatsuji N, Nakahata T. 2007. alpha4-Integrin(+) endothelium derived from primate embryonic stem cells generates primitive and definitive hematopoietic cells. Blood 109:2406–2415.

Sugimoto C, Fujieda S, Sunaga H, Noda I, Tanaka N, Kimura Y, Saito H, Matsukawa S. 2001. Granulocyte colony-stimulating factor (G-CSF)-mediated signaling regulates type IV collagenase activity in head and neck cancer cells. Int J Cancer 93:42–46.

Suwabe N, Takahashi S, Nakano T, Yamamoto M. 1998. GATA-1 regulates growth and differentiation of definitive erythroid lineage cells during in vitro ES cell differentiation. Blood 92:4108–4118.

Takahashi K, Tanabe K, Ohnuki M, Narita M, Ichisaka T, Tomoda K, Yamanaka S. 2007. Induction of pluripotent stem cells from adult human fibroblasts by defined factors. Cell 131:861–872.

Takahashi K, Yamanaka S. 2006. Induction of pluripotent stem cells from mouse embryonic and adult fibroblast cultures by defined factors. Cell 126:663–676.

Toda Y, Kono K, Abiru H, Kokuryo K, Endo M, Yaegashi H, Fukumoto M. 1999. Application of tyramide signal amplification system to immunohistochemistry: a potent method to localize antigens that are not detectable by ordinary method. Pathol Int 49:479–483.

Tulpule A, Lensch MW, Miller JD, Austin K, D'Andrea A, Schlaeger TM, Shimamura A, Daley GQ. 2010. Knockdown of Fanconi anemia genes in human embryonic stem cells reveals early developmental defects in the hematopoietic lineage. Blood 115:3453–3462.

Uchida T, Kanno T, Hosaka S. 1985. Direct measurement of phagosomal reactive oxygen by luminol-binding microspheres. J Immunol Methods 77:55–61.

Umeda K, Heike T, Yoshimoto M, Shinoda G, Shiota M, Suemori H, Luo HY, Chui DH, Torii R, Shibuya M, Nakatsuji N, Nakahata T. 2006. Identification and characterization of hemoangiogenic progenitors during cynomolgus monkey embryonic stem cell differentiation. Stem Cells 24:1348–1358.

Umeda K, Heike T, Yoshimoto M, Shiota M, Suemori H, Luo HY, Chui DH, Torii R, Shibuya M, Nakatsuji N, Nakahata T. 2004. Development of primitive and definitive hematopoiesis from nonhuman primate embryonic stem cells in vitro. Development 131:1869–1879.

van de Winkel JG, Anderson CL. 1991. Biology of human immunoglobulin G Fc receptors. J Leukoc Biol 49:511–524.

van Lochem EG, van der Velden VH, Wind HK, te Marvelde JG, Westerdaal NA, van Dongen JJ. 2004. Immunophenotypic differentiation patterns of normal hematopoiesis in human bone marrow: reference patterns for age-related changes and disease-induced shifts. Cytometry B Clin Cytom 60:1–13.

Vowells SJ, Sekhsaria S, Malech HL, Shalit M, Fleisher TA. 1995. Flow cytometric analysis of the granulocyte respiratory burst: a comparison study of fluorescent probes. J Immunol Methods 178:89–97.

Winterbourn CC. 2002. Biological reactivity and biomarkers of the neutrophil oxidant, hypochlorous acid. Toxicology 181-182:223–227.

Yokoyama Y, Suzuki T, Sakata-Yanagimoto M, Kumano K, Higashi K, Takato T, Kurokawa M, Ogawa S, Chiba S. 2009. Derivation of functional mature neutrophils from human embryonic stem cells. Blood 113:6584–6592.

Yu J, Vodyanik MA, Smuga-Otto K, Antosiewicz-Bourget J, Frane JL, Tian S, Nie J, Jonsdottir GA, Ruotti V, Stewart R, Slukvin II, Thomson JA. 2007. Induced pluripotent stem cell lines derived from human somatic cells. Science 318:1917–1920 .

Chromosome abnormalities in advanced stage T-cell lymphoblastic lymphoma of children and adolescents: a report from Japanese Paediatric Leukaemia/Lymphoma Study Group (JPLSG) and review of the literature

Masahiro Sekimizu,[1] Shosuke Sunami,[2] Atsuko Nakazawa,[3] Yasuhide Hayashi,[4] Yuri Okimoto,[5] Akiko M. Saito,[6] Keizo Horibe,[1,7] Masahito Tsurusawa[8] and Tetsuya Mori[9]

[1]Department of Paediatrics, National Hospital Organization Nagoya Medical Centre, Aichi, [2]Department of Paediatrics, Narita Red Cross Hospital, Chiba, [3]Department of Pathology, National Centre for Child Health and Development, Tokyo, [4]Department of Haematology/Oncology, Gunma Children's Medical Centre, Gunma, [5]Division of Haematology and Oncology, Chiba Children's Hospital, Chiba, [6]Department of Clinical Research Promotion, Clinical Research Centre, National Hospital Organization Nagoya Medical Centre, [7]Clinical Research Centre, National Hospital Organization Nagoya Medical Centre, [8]Department of Paediatrics, Aichi Medical University, Aichi, and [9]Division of Paediatric Oncology, National Centre for Child Health and Development, Tokyo, Japan

Summary

T-cell acute lymphoblastic leukaemia (T-ALL) and T-cell lymphoblastic lymphoma (T-LBL) are combined into one category as T lymphoblastic leukaemia/lymphoma in the current World Health Organization (WHO) classification. However, there is still ongoing discussion on whether T-ALL and T-LBL are two separate entities or represent two variant phenotypes of the same disease. Cytogenetic analysis has been used to identify the molecular background of haematological malignancies. To compare the distribution of chromosomal abnormalities of T-ALL and T-LBL, large series of cytogenetic data are required, but are absent in T-LBL in contrast to the abundant data in T-ALL. Among 111 T-LBL cases in our clinical trial, we obtained complete cytogenetic data from 56 patients. The comparison between our cytogenetic findings and those from three published T-LBL studies revealed no significant difference. However, meta-analysis showed that translocations involving chromosome region 9q34 were significantly more common in T-LBL than in T-ALL. In particular, four out of the 92 T-LBL cases, but none of the 523 paediatric T-ALL cases, showed translocation t(9;17)(q34;q22–23) ($P = 0.0004$). Further studies are needed for the possible linkage between abnormal expression of genes located at 9q34 and/or 17q22–23 and the unique 'lymphoma phenotype' of T-LBL.

Keywords: T-cell lymphoma, child, non-Hodgkin lymphoma, cancer cytogenetics, leukaemia.

In children and adolescents, precursor T lymphoblastic neoplasms have been classified into two diseases: T-cell acute lymphoblastic leukaemia (T-ALL) and T-cell lymphoblastic lymphoma (T-LBL). Although the current World Health Organization (WHO) classification designates both malignancies as T lymphoblastic leukaemia/lymphoma (Borowitz & Chan, 2008), there is continuing discussion on whether T-ALL and T-LBL are two separate entities or whether they represent two different clinical presentations of the same disease. They show overlapping clinical, pathological and immunophenotypic features. In general, the word 'lymphoma' is used if there is a bulky mass in the mediastinum or elsewhere, with less peripheral blood and bone marrow (BM) involvement. Most study groups distinguish between leukaemia and lymphoma on the basis of the extent of BM involvement: patients with <25% lymphoblasts in the BM are diagnosed with lymphoblastic lymphoma; in cases

of 25% or more BM blasts, the diagnosis is leukaemia. While this distinction may appear somewhat arbitrary, a notable observation is that T-LBL patients with large mediastinal masses frequently exhibit little, if any, evidence of tumour dissemination and BM involvement, but the molecular background for this difference is unknown.

Chromosomal analysis has been widely used as a primary step that is required to narrow down the responsible genes that define a disease entity. For instance, discovery of Ph chromosome led to the identification of the chimeric *BCR/ABL1* gene, which is responsible for and defines chronic myeloid leukaemia. Compared with T-ALL, chromosomal abnormalities in T-LBL are not well defined. Reports in the literature and current textbooks claim that the typical chromosomal aberrations reported in T-ALL can also be found in T-LBL (Borowitz & Chan, 2008). However, there are no large series of cytogenetic data on T-LBL (Burkhardt, 2010).

This study aimed to fill the gap regarding cytogenetic data in T-LBL and compare the cytogenetic findings of T-ALL and T-LBL, which may lead to identification of the molecular background behind phenotypical differences between the two disease entities.

Study patients

From November 2004 to October 2010, 154 eligible children (aged 1–18 years) with newly diagnosed advanced stage LBL (Murphy stages III and IV) (Murphy, 1980) were entered in the Japanese Paediatric Leukaemia/Lymphoma Study Group (JPLSG) ALB-NHL03 study (UMIN000002212, http://www.umin.ac.jp/ctr/index-j.htm). Patients with primary immunodeficiencies, Down syndrome and T-cell diseases as second malignancies were excluded. The ethics committee of each participating institute approved the study protocol.

Cytogenetic analysis

Cytogenetic analysis was performed on cell suspensions obtained from 31 tumour/lymph nodes, 19 pleural effusions and six bone marrow samples. The methods of chromosome preparation for cytogenetic analysis are described elsewhere (Sanger *et al*, 1987; Horsman *et al*, 2001). Karyotypes are described according to the International System for Human Cytogenetic Nomenclature (ISCN) (Shaffer & Tommerup, 2005). Only those cases with abnormal cytogenetic study results, defined as two or more cells with the same structural abnormality or the same numerical gain, three or more cells with the same numerical loss or isolated cells with disease-associated abnormalities, were eligible for inclusion in this study.

Statistical methods

Two-tailed Fisher's exact test was used to analyse the patients' characteristics and the frequency of each chromosome abnormality. Significant differences in the analysis of he frequency of

each chromosome abnormality were determined by the two-tailed Fisher's exact test with Bonferroni correction comparison. The *P* value threshold for inclusion of a new variable was chosen to be $P < 0.003$ in this analysis (0.05/17, after Bonferroni correction). A review of T-LBL and T-ALL karyotypes reported in the literature was obtained from a PubMed search and information on chromosome abnormalities and gene fusions was obtained from Mitelman Database of Chromosome Aberrations and Gene Fusions in Cancer (http://cgap.nci.nih.gov/Chromosomes/Mitelman).

Results

Patient characteristics

A total of 154 children were enrolled on JPLSG ALB-NHL03 protocols; 111 cases were T-LBL. Among 111 T-LBL cases, the study population for the current analysis included 56 patients for whom complete cytogenetic data were obtained. With respect to presenting features, patients with reviewed and accepted cytogenetic data were similar to both those without accepted cytogenetic data and the entire cohort of concurrently enrolled T-lineage LBL patients (Table S1).

Frequency of chromosomal abnormalities

Multiple chromosome abnormalities were identified in 31 patients (45%). Structural chromosome abnormalities were identified in 29 patients (52%), and numerical chromosome abnormalities were identified in 18 patients (32%). Ploidy results included pseudodiploid in 14 patients (25%), hypodiploid in three patients (5%), hyperdiploid with 47–50 chromosomes in 10 patients (18%), hyperdiploid with more than 50 chromosomes in four patients (7%) and diploid in 25 patients (45%) (Table S2).

All of the hypodiploid cases had 43–45 chromosomes; none had a near-haploid karyotype. Of the four cases with more than 50 chromosomes, two had near-tetraploid karyotypes. The frequencies of ploidy groups in this series are compared with those reported in other series of karyotyped T-LBL patients and paediatric T-ALL (Table S2). Structural chromosome abnormalities were identified in 29 patients (52%). In the current study, seven patients (13% of those with abnormal karyotypes) exhibited a rearrangement at one or more of the chromosome bands (7p15, 7q32–36 and/or 14q11–13) that are the locations of T-cell receptor chain genes. Rearrangements in the 14q11–13 region, in which the T-cell receptor α/δ chain genes are located, were present in three patients (5%) of the karyotypically abnormal cases in this series (Table S2). Structural abnormalities involving chromosome region 9q34 were identified in nine patients (16%). Translocations involving chromosome region 9q34 were identified in three patients (5%) (t(9;17)(q34;q22), t(7;9)(q34;q34) and t(2;9)(q23;q34)). In comparison between cytogenetic findings in the current data and combined data of three published reports (Burkhardt

et al, 2006; Lones et al, 2007; Uyttebroeck et al, 2007; Table S1), the frequencies of numerical and structural cytogenetic abnormalities in T-LBL and T-ALL had no significant difference (Table S2).

We compared the cytogenetic findings in the current study with the published reports from the three largest-scale studies on T-LBL (Burkhardt et al, 2006; Lones et al, 2007; Uyttebroeck et al, 2007; Table S3) and those from the two largest-scale studies on T-ALL combined (Heerema et al, 1998; Schneider et al, 2000; Table S3) (Table I). The frequencies of almost all of the cytogenetic abnormalities in T-LBL and T-ALL had no significant difference, but translocation involving chromosome region 9q34 was significantly more common in T-LBL than in T-ALL (P = 0·0004, Table S3) and translocation t(9;17) was also more common in T-LBL (4%, 4/92) than in T-ALL (0%, 0/523, P = 0·0004) (Table I).

The current study included a patient with translocation t(9;17)(q34;q22). As far as we could tell from the consulted published reports, all T-LBL patients with translocation t(9;17) presented with a mediastinal mass and without any bone marrow involvement (Kaneko et al, 1988; Shikano et al, 1992) (Table II).

Discussion

This is the largest study involving cytogenetic analysis of T-LBL and the first study to directly compare cytogenetic findings of T-LBL and T-ALL. The frequencies of almost all of the cytogenetic abnormalities in both entities were found to have no significant difference, but translocation involving chromosome region 9q34 was significantly more common in T-LBL than in T-ALL. The current study included a patient with unique translocation t(9;17)(q34;q22). Interestingly, four out of the 92 T-LBL cases, but none of the 523 paediatric T-ALL cases, showed this translocation (P = 0·0004) (Table I). Translocation t(9;17) has been reported in several haematological diseases, such as precursor B-cell ALL (Coyaud et al, 2010), acute myeloid leukaemia (Mrózek et al, 2001), chronic myeloid leukaemia (DeAngelo et al, 2004), chronic lymphocytic leukaemia (Michaux et al, 2005), diffuse large B-cell lymphoma (Hammond et al, 1992) and follicular lymphoma (Aamot et al, 2007), but these breakpoints, 9q34 and 17q22–23, are limited in the cases of T-LBL (http://cgap.nci.nih.gov/Chromosomes/Mitelman). These results imply a linkage between abnormal expression of genes located at 9q34 and/or 17q22–23 and the unique phenotypes of the T-LBL mentioned above.

Cytogenetic analysis has been used to identify the molecular background of haematological malignancies. To compare the distribution of chromosomal abnormalities of T-ALL and T-LBL, large series of cytogenetic data are required, but are absent in T-LBL in contrast to the abundant data in T-ALL. Three recent series of cytogenetic data on paediatric T-LBL have been published, reporting the cytogenetic findings in 13, 11 and 12 paediatric T-LBL cases (Burkhardt et al, 2006; Lones

Table I. Comparison of cytogenetic findings between T-LBL and T-ALL.

	T-LBL		T-ALL		
	n	%	n	%	P value
Total	92		523		
Normal karyotype†	36	39	219	42	0·6478
Abnormal karyotype	56	61	304	58	0·6478
Hypodiploid	4	4	20	4	0·9999
Pseudodiploid	30	33	204	39	0·2000
Hyperdiploid(47–50)	18	20	64	12	0·0328
Hyperdiploid(>50)	4	4	16	3	0·5217
Any translocation	26	28	177	34	0·3367
Any del chrome.	19	21	160	31	0·0328
Any der chrome.	4	4	58	11	0·0583
del(6q)	6	7	69	13	0·0833
Loss of 9p	10	11	44	8	0·5487
Any 14q11–13 abnormality	10	11	72	14	0·5100
Any 7q32–36 abnormality	7	8	35	7	0·8220
Any translocation including 9q34	8	9	7	1	0·0004*
t(7;10)	1	1	2	0	0·3855
t(10;11)	1	1	8	2	0·9999
t(9;17)	4	4	0	0	0·0004*

†Includes one Klinefelter syndrome, and one inv(9) without other abnormality in current report.
The P value threshold for inclusion of a new variable was chosen to be 0·003 (0·05/17, after Bonferroni correction). *P < 0·003.
T-LBL: current study (JPLSG ALB-NHL03) combined with three published reports(Burkhardt et al, 2006; Lones et al, 2007; Uyttebroeck et al, 2007).
T-ALL: combined two published reports (Heerema et al, 1998; Schneider et al, 2000).

et al, 2007; Uyttebroeck et al, 2007). Thus, this study can play a role to fill the gap of cytogenetic data on T-LBL.

Translocation involving chromosome region 9q34 was found to be significantly more common in T-LBL than in T-ALL (Table I). Among genes located in the 9q34 region, SET, PKN3, ABL1, NUP214 and NOTCH1 have previously been implicated in malignancy, with SET, ABL1, NUP214 and NOTCH1 being implicated in leukemogenesis (Ellisen et al, 1991; van Vlierberghe et al, 2008; Hagemeijer & Graux, 2010).

An oncogenic SET-NUP214 fusion gene has been reported in a case of acute undifferentiated leukaemia with a reciprocal translocation t(9;9)(q34; q34) (von Lindern et al, 1992) and NK adult acute myeloid leukaemia as a result of a cryptic deletion of 9q34 (Rosati et al, 2007). van Vlierberghe et al (2008) identified the SET-NUP214 fusion gene in three patient samples out of 92 paediatric cases of T-cell leukaemia. SET-NUP214 may contribute to T-ALL pathogenesis by inhibition of T-cell maturation through the transcriptional activation of the HOXA genes (van Vlierberghe et al, 2008). However, the frequency of this mutation in T-LBL is unknown.

NOTCH1, previously termed TAN1, was discovered as a partner gene in T-ALL with a translocation t(7;9)(q34;q34.3), and was found in <1% of T-ALLs (Ellisen et al, 1991). Several

Table II. Clinical characteristics and detailed karyotype data in T-LBL patients with t(9;17).

	Age (years)	Sex	Tumour site	Stage	BM blast %	Karyotype
Kaneko et al (1988)	14	F	Mediastinum	III	0	46,XX,t(9;17)(q34;q23)
	15	M	Mediastinum	III	0	46,XY,-9,del(6)(q13q21),t(9;17)(q34;q23),+der(9)t(9;17)(q34;q23)
	10	M	Mediastinum	III	0	47,XY,+19,t(9;17)(q34;q23)
Shikano et al (1992)	14	F	Mediastinum	III	0	46,XX,t(9;17)(q34;q23)
	7	M	Mediastinum	III	0	49,XY-1,+der(l)t(l;?)(p36;?),t(9;17)(q34;q23),+14,+marl,+mar2
	5	F	Mediastinum	III	0	47,XX,t(9;17)(q34;q23),+der(17)t(9;17)(q34;q23)
Burkhardt et al (2006)	ND	ND	ND	ND	ND	46,XX,del(6)(q1?2q1?6),t(9;17)(q34;q22)
	ND	ND	ND	ND	ND	47,XX,t(9;17)(q34;q22),+20
Lones et al (2007)	8	M	Mediastinum	III	0	47,XY,t(9;17)(q3?4;q2?3),+20
Current study	7	M	Mediastinum	III	0	46,XY,t(9;17)(q34;q22)

ND, no data available.

study groups reported NOTCH1 mutations in 31–62% of T-ALL patients (Weng et al, 2004; Breit et al, 2006; van Grotel et al, 2006; Zhu et al, 2006; Malyukova et al, 2007; Asnafi et al, 2009; Gedman et al, 2009; Park et al, 2009). In contrast, only two studies reported NOTCH1 mutation analyses in T-LBL: Park et al (2009) reported NOTCH1 mutations in six out of 14 paediatric T-LBL patients (43%), and Baleydier et al (2008) reported mutations in six out of nine paediatric T-LBL (66%), with 32 adult patients with NOTCH1 mutations in 16 cases (54% in all patients) (Baleydier et al, 2008). According to these reports, the frequencies of NOTCH1 mutation were not significantly different between T-LBL and T-ALL.

ABL1 fusion genes have been identified that provide proliferation and survival advantage to lymphoblasts. NUP214-ABL1, EML1-ABL1, BCR-ABL1 and ETV6-ABL1 chimeric genes have been reported. The most frequent one in T-ALL is the NUP214-ABL1 fusion gene, which has been identified in 6% of cases, in both children and adults (Graux et al, 2009). In addition, using an oligonucleotide microarray, ABL1 overexpression was identified in 8% of cases in T-ALL (Chiaretti et al, 2007). Our review of these published reports indicated that the frequency of ABL1 mutation in T-LBL is unknown.

Raetz et al (2006) analysed the gene expression profiles of ten T-ALL BM samples and nine T-LBL samples using a microarray. They identified 133 genes for which the expression levels differed between T-LBL and T-ALL. ZNF79 (encoding zinc finger protein 79) and ABL1, both located in chromosome region 9q34, were included in these genes and showed at least twofold higher overexpression in T-LBL than that in T-ALL. Additionally, MED13 (previously termed THRAP1), which is located in 17q22-q23, also showed at least twofold higher overexpression in T-LBL than that in T-ALL (Raetz et al, 2006). Taking these findings together, it is possible that ZNF79, ABL1 or THRAP1 as well as other genes at 9q34 and 17q22–23 are involved in the 'lymphoma phenotype' such as a bulky mass in the mediastinum and minimal BM involvement. These findings need further study to determine if this linkage constitutes a unique 'lymphoma phenotype'.

Authorship

MS designed the study, prepared the data file, performed the analysis, interpreted data and wrote the manuscript. SS is a lead principal investigator for the JPLSG ALB-NHL03 study. AN contributed to pathological diagnosis. YH contributed to chromosome analysis. YO is a principal investigator contributing a patient to this study. AMS contributed to statistical analysis. KH received a research grant from the Ministry of Health, Labour and Welfare of Japan. MT is a chairperson of JPLSG. TM is a chairperson of JPLSG lymphoma committee. SS, KH, MT and TM were primarily responsible for the study design, data analysis and interpretation of the data. All authors approved the final manuscript.

Disclosure

The authors declare no competing financial interests.

Supporting Information

Additional Supporting Information may be found in the online version of this article:

Table S1. Respective clinical characteristics with and without karyotype data in 111 T-LBL patients in the current study.

Table S2. Comparison of cytogenetic findings in T-LBL between current study and combined data of three published reports.

Table S3. Published data of cytogenetic findings in T-LBL and T-ALL.

Please note: Wiley-Blackwell are not responsible for the content or functionality of any supporting materials supplied by the authors. Any queries (other than missing material) should be directed to the corresponding author for the article.

References

Aamot, H.V., Torlakovic, E.E., Eide, M.B., Holte, H. & Heim, S. (2007) Non-Hodgkin lymphoma with t(14;18): clonal evolution patterns and cytogenetic-pathologic-clinical correlations. *Journal of Cancer Research and Clinical Oncology*, 133, 455–470.

Asnafi, V., Buzyn, A., Le Noir, S., Baleydier, F., Simon, A., Beldjord, K., Reman, O., Witz, F., Fagot, T., Tavernier, E., Turlure, P., Leguay, T., Huguet, F., Vernant, J.P., Daniel, F., Bene, M.C., Ifrah, N., Thomas, X., Dombret, H. & Macintyre, E. (2009) NOTCH1/FBXW7 mutation identifies a large subgroup with favorable outcome in adult T-cell acute lymphoblastic leukemia (T-ALL): a Group for Research on Adult Acute Lymphoblastic leukemia (GRAALL) study. *Blood*, 113, 3918–3924.

Baleydier, F., Decouvelaere, A.V., Bergeron, J., Gaulard, P., Canioni, D., Bertrand, Y., Lepretre, S., Petit, B., Dombret, H., Beldjord, K., Molina, T., Asnafi, V. & Macintyre, E. (2008) T cell receptor genotyping and HOXA/TLX1 expression define three T lymphoblastic lymphoma subsets which might affect clinical outcome. *Clinical Cancer Research*, 14, 692–700.

Borowitz, M. & Chan, J. (2008) WHO Classification of Tumours of Haematopoietic and Lymphoid Tissues. In: T lymphoblatic leukaemia/lymphoma (ed. by S. Swerdlow, E. Campo, N. Harris, E. Jaffe, S. Pileri, H. Stein, J. Thiele & J. Vardiman), pp. 176–178. Internationa Agency for Resarchon Cancer, Lyon.

Breit, S., Stanulla, M., Flohr, T., Schrappe, M., Ludwig, W.D., Tolle, G., Happich, M., Muckenthaler, M.U. & Kulozik, A.E. (2006) Activating NOTCH1 mutations predict favorable early treatment response and long term outcome in child-hood precursor T-cell lymphoblastic leukemia. *Blood*, 108, 1151–1157.

Burkhardt, B. (2010) Paediatric lymphoblastic T-cell leukaemia and lymphoma: one or two diseases? *British Journal of Haematology*, 149, 653–668.

Burkhardt, B., Bruch, J., Zimmermann, M., Strauch, K., Parwaresch, R., Ludwig, W.D., Harder, L., Schlegelberger, B., Mueller, F., Harbott, J. & Reiter, A. (2006) Loss of heterozygosity on chromosome 6q14-q24 is associated with poor outcome in children and adolescents with T-cell lymphoblastic lymphoma. *Leukemia*, 20, 1422–1429.

Chiaretti, S., Tavolaro, S., Ghia, E.M., Ariola, C., Matteucci, C., Elia, L., Maggio, R., Messina, M., Ricciardi, M.R., Vitale, A., Ritz, J., Mecucci, C., Guarini, A. & Foa, R. (2007) Characterization of ABL1 expression in adult T-cell acute lymphoblastic leukemia by oligonucleotide array analysis. *Haematologica*, 92, 619–626.

Coyaud, E., Struski, S., Prade, N., Familiades, J., Eichner, R., Quelen, C., Bousquet, M., Mugneret, F., Talmant, P., Pages, M.P., Lefebvre, C., Penther, D., Lippert, E., Nadal, N., Taviaux, S., Poppe, B., Luquet, I., Baranger, L., Eclache, V., Radford, I., Barin, C., Mozziconacci, M.J., Lafage-Pochitaloff, M., Antoine-Poirel, H., Charrin, C., Perot, C., Terre, C., Brousset, P., Dastugue, N. & Broccardo, C. (2010) Wide diversity of PAX5 alterations in B-ALL: a Groupe Francophone de Cytogenetique Hematologique Study. *Blood*, 115, 3089–3097.

DeAngelo, D.J., Hochberg, E.P., Alyea, E.P., Longtine, J., Lee, S., Galinsky, I., Parekkedon, B., Ritz, J., Antin, J.H., Stone, R.M. & Soiffer, R.J. (2004) Extended follow-up of patients treated with imatinib mesylate (gleevec) for chronic myelogenous leukemia relapse after allogeneic transplantation: durable cytogenetic remission and conversion to complete donor chimerism without graft-versus-host disease. *Clinical Cancer Research*, 10, 5065–5071.

Ellisen, L.W., Bird, J., West, D.C., Soreng, A.L., Reynolds, T.C., Smith, S.D. & Sklar, J. (1991) TAN-1, the human homolog of the Drosophila notch gene, is broken by chromosomal translocations in T lymphoblastic neoplasms. *Cell*, 66, 649–661.

Gedman, A.L., Chen, Q., Kugel Desmoulin, S., Ge, Y., Lafiura, K., Haska, C.L., Cherian, C., Devidas, M., Linda, S.B., Taub, J.W. & Matherly, L.H. (2009) The impact of NOTCH1, FBW7 and PTEN mutations on prognosis and downstream signaling in paediatric T-cell acute lymphoblastic leukemia: a report from the Children's Oncology Group. *Leukemia*, 23, 1417–1425.

Graux, C., Stevens-Kroef, M., Lafage, M., Dastugue, N., Harrison, C.J., Mugneret, F., Bahloula, K., Struski, S., Gregoire, M.J., Nadal, N., Lippert, E., Taviaux, S., Simons, A., Kuiper, R.P., Moorman, A.V., Barber, K., Bosly, A., Michaux, L., Vandenberghe, P., Lahortiga, I., de Keersmaecker, K., Wlodarska, I., Cools, J., Hagemeijer, A. & Poirel, H.A. (2009) Heterogeneous patterns of amplification of the NUP214-ABL1 fusion gene in T-cell acute lymphoblastic leukemia. *Leukemia*, 23, 125–133.

van Grotel, M., Meijerink, J.P., Beverloo, H.B., Langerak, A.W., Buys- Gladdines, J.G., Schneider, P., Poulsen, T.S., den Boer, M.L., Horstmann, M., Kamps, W.A., Veerman, A.J., van Wering, E.R., van Noesel, M.M. & Pieters, R. (2006) The outcome of molecularcytogenetic subgroups in pediatric T-cell acute lymphoblastic leukemia: a retrospective study of patients treated according to DCOG or COALL protocols. *Haematologica*, 91, 1212–1221.

Hagemeijer, A. & Graux, C. (2010) ABL1 rearrangements in T-cell acute lymphoblastic leukemia. *Genes, Chromsomes & Cancer*, 59, 299.

Hammond, D.W., Goepel, J.R., Aitken, M., Hancock, B.W., Potter, A.M. & Goyns, M.H. (1992) Cytogenetic analysis of a United Kingdom series of non-Hodgkins lymphomas. *Cancer Genetics and Cytogenetics*, 61, 31–38.

Heerema, N.A., Sather, H.N., Sensel, M.G., Kraft, P., Nachman, J.B., Steinherz, P.G., Lange, B.J., Hutchinson, R.S., Reaman, G.H., Trigg, M.E., Arthur, D.C., Gaynon, P.S. & Uckun, F.M. (1998) Frequency and clinical significance of cytogenetic abnormalities in pediatric T-lineage acute lymphoblastic leukemia: a report from the Children's Cancer Group. *Journal of Clinical Oncology*, 16, 1270–1278.

Horsman, D.E., Connors, J.M., Pantzar, T. & Gascoyne, R.D. (2001) Analysis of secondary chromosomal alterations in 165 cases of follicular lymphoma with t(14;18). *Genes, Chromosomes and Cancer*, 30, 375–382.

Kaneko, Y., Frizzera, G., Maseki, N., Sakurai, M., Komada, Y., Hiyoshi, Y., Nakadate, H. & Takeda, T. (1988) A novel translocation, t(9;17)(q34;q23), in aggressive childhood lymphoblastic lymphoma. *Leukemia*, 2, 745–748.

von Lindern, M., Breems, D., van Baal, S., Adriaansen, H. & Grosveld, G. (1992) Characterization of the translocation breakpoint sequences of two DEK-CAN fusion genes present in t(6;9) acute myeloid leukaemia and a SET-CAN fusion gene found in a case of acute undifferentiated leukemia. *Genes, Chromosomes and Cancer*, 5, 227–234.

Lones, M.A., Heerema, N.A., Le Beau, M.M., Sposto, R., Perkins, S.L., Kadin, M.E., Kjeldsberg, C.R., Meadows, A., Siegel, S., Buckley, J., Abromowitch, M., Kersey, J., Bergeron, S., Cairo, M.S. & Sanger, W.G. (2007) Chromosome abnormalities in advanced stage lymphoblastic lymphoma of children and adolescents: a report from CCG-E08. *Cancer Genetics and Cytogenetics*, 172, 1–11.

Malyukova, A., Dohda, T., von der Lehr, N., Akhoondi, S., Corcoran, M., Heyman, M., Spruck, C., Grander, D., Lendahl, U. & Sangfelt, O. (2007) The tumor suppressor gene hCDC4 is frequently mutated in human T-cell acute lymphoblastic leukemia with functional consequences for Notch signaling. *Cancer Research*, 67, 5611–5616.

Michaux, L., Wlodarska, I., Rack, K., Stul, M., Criel, A., Maerevoet, M., Marichal, S., Demuynck, H., Mineur, P., Kargar Samani, K., Van Hoof, A., Ferrant, A., Marynen, P. & Hagemeijer, A. (2005) Translocation t(1;6)(p35.3;p25.2): a new recurrent aberration in "unmutated" B-CLL. *Leukemia*, 19, 77–82.

Mrózek, K., Prior, T.W., Edwards, C., Marcucci, G., Carroll, A.J., Snyder, P.J., Koduru, P.R.K., Theil, K.S., Pettenati, M.J., Archer, K.J., Caligiuri, M.A., Vardiman, J.W., Kolitz, J.E., Larson, R.A. & Bloomfield, C.D. (2001) Comparison of cytogenetic and molecular genetic detection of t(8;21)

and inv(16) in a prospective series of adults with de novo acute myeloid leukaemia: a Cancer and leukemia Group B study. *Journal of Clinical Oncology*, **19**, 2482–2492.

Murphy, S. (1980) Classification, staging, and end results of treatment of childhood non-Hodgkin's lymphomas: dissimilarities from lymphomas in adults. *Seminars in Oncology*, **7**, 332–339.

Park, M.J., Taki, T., Oda, M., Watanabe, T., Yumura-Yagi, K., Kobayashi, R., Suzuki, N., Hara, J., Horibe, K. & Hayashi, Y. (2009) FBXW7 and NOTCH1 mutations in childhood T cell acute lymphoblastic leukaemia and T cell non-Hodgkin lymphoma. *British Journal of Haematology*, **145**, 198–206.

Raetz, E.A., Perkins, S.L., Bhojwani, D., Smock, K., Philip, M., Carroll, W.L. & Min, D.J. (2006) Gene expression profiling reveals intrinsic differences between T-cell acute lymphoblastic leukemia and T-cell lymphoblastic lymphoma. *Pediatric Blood and Cancer*, **47**, 130–140.

Rosati, R., La Starza, R., Barba, G., Gorello, P., Pierini, V., Matteucci, C., Roti, G., Crescenzi, B., Aloisi, T., Aversa, F., Martelli, M.F. & Mecucci, C. (2007) Cryptic chromosome 9q34 deletion generates TAF-Iα/CAN and TAF-Iβ/CAN fusion

transcripts in acute myeloid leukemia. *Haematologica*, **92**, 232–235.

Sanger, W.G., Armitage, J.O., Bridge, J., Weisenburger, D.D., Fordyce, R. & Purtilo, D.T. (1987) Initial and subsequent cytogenetic studies in malignant lymphoma. *Cancer*, **60**, 3014–3019.

Schneider, N.R., Carroll, A.J., Shuster, J.J., Pullen, D.J., Link, M.P., Borowitz, M.J., Camitta, B.M., Katz, J.A. & Amylon, M.D. (2000) New recurring cytogenetic abnormalities and association of blast cell karyotypes with prognosis in childhood T-cell acute lymphoblastic leukemia: a pediatric oncology group report of 343 cases. *Blood*, **96**, 2543–2549.

Shaffer, L.G. & Tommerup, N. (2005) *ISCN (2005) an International System for Human Cytogenetic Nomenclature*. S. Karger, Basel.

Shikano, T., Ishikawa, Y., Naito, H., Kobayashi, R., Nakadate, H., Hatae, Y. & Takeda, T. (1992) Cytogenetic characteristics of childhood non-Hodgkin lymphoma. *Cancer*, **70**, 714–719.

Uyttebroeck, A., Vanhentenrijk, V., Hagemeijer, A., Boeckx, N., Renard, M., Wlodarska, I., Vandenberghe, P., Depaepe, P. & de Wolf-Peeters, C. (2007) Is there a difference in childhood T-cell acute lymphoblastic leukemia and T-cell

lymphoblastic lymphoma? *Leukemia & Lymphoma*, **48**, 1745–1754.

van Vlierberghe, P., van Grotel, M., Tchinda, J., Lee, C., Beverloo, H.B., van der Spek, P.J., Stubbs, A., Cools, J., Nagata, K., Fornerod, M., Buijs-Gladdines, J., Horstmann, M., van Wering, E.R., Soulier, J., Pieters, R. & Meijerink, J.P. (2008) The recurrent SET-NUP214 fusion as a new HOXA activation mechanism in pediatric T-cell acute lymphoblastic leukemia. *Blood*, **111**, 4668–4680.

Weng, A.P., Ferrando, A.A., Lee, W., Morris, J.P., Silverman, L.B., Sanchez-Irizarry, C., Blacklow, S.C., Look, A.T. & Aster, J.C. (2004) Activating mutations of NOTCH1 in human T cell acute lymphoblastic leukemia. *Science*, **306**, 269–271.

Zhu, Y.M., Zhao, W.L., Fu, J.F., Shi, J.Y., Pan, Q., Hu, J., Gao, X.D., Chen, B., Li, J.M., Xiong, S.M., Gu, L.J., Tang, J.Y., Liang, H., Jiang, H., Xue, Y.Q., Shen, Z.X., Chen, Z. & Chen, S.J. (2006) NOTCH1 mutations in T-cell acute lymphoblastic leukaemia: prognostic significance and implication in multifactorial leukemogenesis. *Clinical Cancer Research*, **12**, 3043–3049.